UNIVERSITY OF NAPLES FEDERICO II

PH.D. PROGRAM IN

CLINICAL AND EXPERIMENTAL MEDICINE

CURRICULUM IN CARDIOVASCULAR AND GERONTOLOGICAL SCIENCES

XXXII Cycle
(Years 2017-2020)

Chairman: Prof. Francesco Beguinot

Ph.D. Thesis

IMPAIRED RIGHT AND LEFT VENTRICULAR FUNCTION IN PATIENTS WITH FIBROTIC INTERSTITIAL LUNG DISEASES

TUTOR

PH.D. STUDENT

Prof. Maurizio Galderisi

Dr. Agostino Buonauro

Impaired right and left ventricular function in patients with fibrotic interstitial lung diseases

Agostino Buonauro MD[1], Ciro Santoro MD[1], Angelo Canora MD[2], Regina Sorrentino MD[1], Roberta Esposito MD, PhD[1], Maria Lembo MD[1], Ludovica Fiorillo MD[2], Mario Canonico MD[1], Maurizio Galderisi MD[1], Alessandro Sanduzzi MD[2], Maria Luisa Bocchino MD[2]

Short title:
Right and left ventricular function in patients with pulmonary fibrosis

(1) DEPARTMENT OF ADVANCED BIOMEDICAL SCIENCES
FEDERICO II UNIVERSITY HOSPITAL,
(2) DEPARTMENT OF CLINICAL MEDICINE AND SURGERY
FEDERICO II UNIVERSITY, MONALDI HOSPITAL,
NAPLES, ITALY

No conflict of interest to declare

Abstract

Background: Interstitial lung diseases (ILDs) include idiopathic (IPF) and no idiopathic pulmonary fibrosis (no-IPF). While left ventricular (LV) and right ventricular (RV) dysfunction is known in IPF, little is known about cardiac involvement in no-IPF. This issue can be explored by advanced echocardiography.

Methods: Sixty-one clinically stable and therapy-naïve fibrotic ILDs patients - 33 IPF and 28 no-IPF, and 30 healthy controls were enrolled after excluding patients with coronary artery disease, overt heart failure, primary cardiomyopathies, other forms of diffuse parenchymal lung disease, history of pulmonary embolism and primary pulmonary arterial hypertension(PAH). ILDs diagnosis was made by chest radiography, spirometry and chest high-resolution computed tomography. Lung cumulative damage was evaluated by diffusion capacity of the lung for carbon monoxide ($DLCO_{sb}$). All patients underwent a complete echo-Doppler exam including 2D quantitation of global longitudinal strain (GLS) of both ventricles and of RV ejection fraction (EF) by 3D echo.

Results: Our findings demonstrated LV diastolic dysfunction in both IPF and no-IPF patients, whilst a subclinical reduction of LV GLS - but not of LV EF - was found only in PF patients. An alteration of and diastolic function and of RV GLS was observed in IPF in comparison with both controls and no-IPF. An association between $DLCO_{sb}$ and RV GLS was found in the pooled ILDs population and in IPF, it being independent on confounders including pulmonary arterial systolic pressure.

Conclusion: These findings point out the diagnostic capabilities of strain imaging in distinguishing early cardiac damage of IPF from and no-IPF patients, a task which cannot be attributed to both standard and 3D echocardiography.

Key words: Interstitial lung diseases, Idiopathic pulmonary fibrosis, Speckle Tracking Echocardiography, Global longitudinal strain, Pulmonary hypertension

Introduction

Interstitial lung diseases (ILDs) include more than 200 disorders, characterized by a variable degree of inflammation and fibrosis leading to an often irreversible loss of lung function, wide spectrum in the clinical course, treatment and prognosis. ILDS can be broadly divided in those without any identifiable cause, i.e., idiopathic pulmonary fibrosis (IPF) and those with identifiable factors such as environmental/occupational exposure, infections, autoimmune systemic diseases, drugs and radiations, which are commonly defined as non-IPF [1]. Among the idiopathic interstitial pneumonia, idiopathic pulmonary fibrosis (IPF) is the most common form, affecting 30 persons per 100.000 in the general population, and as many as 175 persons per 100.000 in the age group of >75 years [2]. Despite recent advances in pharmacotherapy [3], IPF is a poor prognosis disease, with a rapidly progressive and debilitating clinical progression [4,5].

Because of its worse prognosis and challenging treatment, pneumological and cardiac aspects of IPF has been deeply investigated. In IPF, the combination of severe vascular and fibrotic disease induces changes in right ventricular (RV) structure and development of RV dysfunction and heart failure [1]. Respiratory function declines along with disease progression, and changes in lung diffusion capacity of carbon monoxide (DLCO) and forced vital capacity (FVC) are both independent predictors of worse prognosis [1]. Pulmonary arterial hypertension (PAH) is frequently found in the early stages of IPF and the outcome of IPF is directly related to the capacity of RV function to adapt to the elevated afterload [6].RV enlargement and dysfunction, as valuated by standard echocardiography, have been well described in IPF patients and can be used to identify patients with high-risk of death [7]. Also an impaired left ventricular (LV) diastolic filling was also observed, whereas LV systolic function appears to be preserved [8]. Speckle Tracking Echocardiography (STE) has also shown to be suitable for diagnosing cardiac dysfunction in IPF patients [9,10]. However, LV and RV function have been poorly explored by advanced echo

technologies in no-IPF and no comparison of strain and 3D imaging exists between IPF and no-IPF patients. Accordingly, the aim of the present study was to analyze LV and RV function and structure in patients with fibrotic ILDs, including both IPF and no-IPF cases, by applying 2D strain to both ventricles and 3D to the right ventricle. Relationships between cardiac parameters and lung function were also evaluated.

Methods

Study population

The study population included 61 patients with clinically stable and therapy-naïve fibrotic ILDs, referred at the time of first diagnosis to the Respiratory Diseases Division of the Federico II University, Monaldi Hospital (Naples, Italy), between October 2016 and October 2018. Thirty-three patients were affected by IPF (IPF group) and 28 had fibrotic ILDs other than IPF (no-IPF group), including idiopathic non-specific interstitial pneumonia (n=14), chronic hypersensitivity pneumonia (n=9), and smoking-related desquamative interstitial pneumonia (n=5). Diagnosis of IPF was made according to the 2011 international diagnostic criteria [2]. Exclusion criteria were coronary artery disease and previous myocardial infarction, more than mild valvular heart disease, congestive heart failure, primary cardiomyopathies, atrial fibrillation, congenital heart disease and inadequate imaging quality. Patients with acute exacerbation of the underlying ILDs and those with concomitant chronic obstructive lung disease were excluded as well. Thirty healthy subjects matched for age and sex, referred for voluntary cardiovascular screeningto the Interdepartmental Laboratory of Echocardiography of the Federico II University (Naples, Italy), entered the study as the control group.

Table 1. Clinical features and baseline heart and lung function parameters of the study population.

Variable	IPF (n=33)	No- IPF (n=28)	p_a	Controls (n=30)	p_b	p_c
Gender (F/M)	6/27	10/18	-	11/19	-	-
Age (years)	70.1 ± 7.6	65.2 ± 8.1	0.067	66.9 ± 8.7	0.375	1.0
BMI (kg/m^2)	27.8 ± 3.8	30.1 ± 4.0	0.068	25.2 ± 3.2	**0.015**	**<0.0001**
Systolic BP (mmHg)	138.8 ± 18.6	133.7 ± 15.2	0.642	128.4 ± 12.5	**0.033**	0.618
Diastolic BP (mmHg)	78.9 ± 12.2	77.5 ± 9.8	1.0	78.7 ± 9.3	1.0	1.0
Heart rate (bpm)	76.8 ± 11.5	75.7 ± 10.9	1.0	68.2 ± 11.1	**0.009**	**0.039**
PaO_2(mm Hg) in ambient air	71.6 ± 10.1	73.1 ±8.7	0.548	-	-	-
$PaCO_2$(mm Hg) in ambient air	39.7 ± 3.7	38.1±3.0	0.327	-	-	-
FVC (%pred)	71.1 ± 20.9	70.6±19.4	0.227	-	-	-
TLC (%pred)	70.9 ± 47.8	70.1±25.9	0.368	-	-	-
DLCO$_{sb}$(%pred)	44.3 ± 17.6	54.7 ±22.3	0.242	-	-	-

p_a= IPF vs non-IPF, p_b= IPF vs controls, p_c:= non- IPF vs controls.

IPF = Idiopathic pulmonary fibrosis, BMI = body mass index, BP = Blood pressure, PaO_2 = Arterial oxygen partial pressure, $PaCO_2$ = Arterial carbon dioxide partial pressure, FVC % = Forced vital capacity, FEV1% = Forced expiratory volume in 1 s, TLC = Total lung capacity; DlCO $_{sb}$ = Single-breath lung diffusion capacity of carbon monoxide.

The study was conducted in accordance with the amended Declaration of Helsinki and approved by the Institutional Ethical Committee (Protocol 1129, 4 August 2015). All patients gave their written informed consent at enrollment. Patients data were collected in an anonymous way.

Lung function evaluation

Spirometry, lung volumes measurement and determination of the haemoglobin (Hb)-adjusted single-breath diffusing lung capacity of the carbon monoxide (DLCOsb) were performed using a computer-assisted spirometer (Quark PFT 2008 Suite Version Cosmed Ltd Rome Italy) according to international standards [11-13]. Arterial gas analysis was performed at rest while patients were breathing ambient air. The 6-minute walk test (6-MWT) was performed by trained hospital staff according to international guidelines [14].
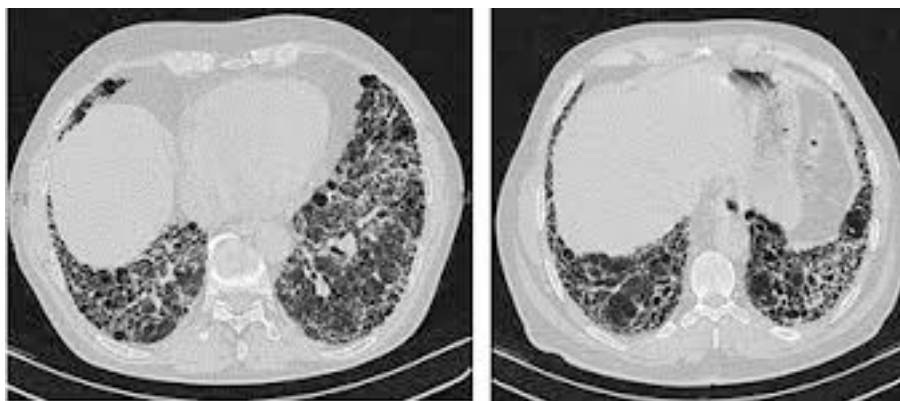
Echocardiographic examination

Standard echo-Doppler exam, including STE of both ventricles and 3D echo of the right ventricle were performed by a Vivid E9 ultrasound machine (GE Healthcare, Horten, Norway), using a 2.5 MHz transducer with harmonic capability, according to the standards of our laboratory

[15-17] and the echo report standardization of the European Association of Cardiovascular Imaging (EACVI) [18]. Blood pressure (BP) and heart rate were measured at the end of each echo exam.

LV quantitative analysis was performed according to guidelines [19]. Relative wall thickness and LV mass were computed by two-dimensional guided M-mode imaging or directly from two-dimensional parasternal long-axis view. Left atrial (LA) volume and LV mass were indexed for body surface area [19]. LV mass index >95 g/m2in women and >115 g/m2in men defined the presence of clear-cut LVH.LV ejection fraction (EF) was computed by measuring LV end-diastolic and end-systolic volumes with the biplane method in apical 4- and 2-chamber view [19]. For the evaluation of diastolic function, Doppler derived transmitral inflow early (E) and atrial (A) peak velocities (m/s), E/A ratio, E velocity deceleration time (DT), pulsed tissue Doppler of septal and lateral annulus early diastolic velocity (e'), average E/e' ratio and tricuspid regurgitation (TR) jet peak velocity were determined in apical 4-chamber view according to current recommendations [20,21]. LV STE acquisition was obtained in the three apical views (long-axis, 4-chamber and 2-chamber) according to the standards of our laboratory [22,23]. Post-processing was performed off-line, on a dedicated work-station (EchoPAC only software version113, GE Healthcare, Chicago, Illinois USA). The tracing of endocardial and epicardial borders was defined using automated 2D strain software, with possible manual readjustment when needed. Peak longitudinal strain was measured from 6 segments in each of the three apical views, and global longitudinal strain (GLS)derived as the average of the individual peak strain before the aortic valve closure. Reproducibility of GLS in our laboratory has been recently reported [23,24].

In a non-foreshortened apical 4-chamber view oriented to obtain the maximal RV internal chamber size, RV diameters (transverse basal and mid-cavity diameters and longitudinal diameter) were measured at end-diastole. RV global systolic function was assessed by measuring tricuspid

annular systolic excursion (TAPSE, mm) by M-mode echo. Pulsed Doppler RV inflow was recorded to measure tricuspid early diastolic (E) and atrial (A) peak velocities (m/sec) and E/A ratio [19]. Pulmonary arterial systolic pressure (PASP) was estimated according to guidelines, based on the TR peak velocity and adding an estimate of right atrial pressure (RAP) by measuring the size and respiratory reactivity of the inferior vena cava (IVC): a) normal RAP (≈ 5 mmHg) based on a normal IVC size (IVC diameter <2.1 cm) with normal inspiratory collapse (>50% decrease in IVC diameter); b) RAP ≈ 10 mmHg: dilated IVC (diameter >2.1 cm) or <50% collapse; c) RAP ≈ 15 mmHg: both dilated IVC and <50% collapse; d) RAP ≈ 20 mmHg: dilated IVC without visible collapse [20]. The cut-off point of PAH was established for an estimated PAPS>30 mmHg. RV GLS was determined by off-line post-processing by averaging values of the 6 segments: 3 of free lateral wall and 3 of interventricular septal wall [15,25].

LV and RV GLS values were considered positive (sign +) to strengthen the clinical meaning: the higher the values, the better is the strain deformation.

3D Echocardiography

3D echocardiographic examination of the right ventricle was performed and analyzed according to previously described procedures [26,27]. A full-volume scan was acquired by harmonic imaging from an apical approach, using a frame rate (in volume per second) higher than 40% of the individual heartbeat or greater 25 frame per second. Four ECG-gated consecutive heart beats were acquired during an end-expiratory apnea (multi-beat acquisition) to generate the full volume. The quality of acquisition was verified in 12-slice display mode in order to exclude stitching artifacts and to ensure the entire RV cavity and walls were included in the full volume and optimal RV border visualization. Adequate data sets were stored digitally in raw data format and exported to EchoPAC only software version 113 (GE Healthcare) and elaborated with a commercially available software (4D RV-Function, TomTec Imaging Systems, Gmbh,

Unterschleissheim, Germany) for off-line analysis. Every RV full-volume3D dataset was automatically cropped in three standard planes (views): 4-chamber, coronal, and sagittal. Endocardial border was traced at end-diastole and end-systole for the 3 selected RV planes and served for initiation of automated border detection algorithm. RV contours were automatically traced over the entire cardiac cycle providing quantification of RV end-diastolic volume, RV end-systolic volumes (RV EDV and ESV respectively) and RVEF. 3D measurements of RV function have been demonstrated to be highly reproducible in our laboratory [28].

Statistical analysis

Statistical analysis was performed by SPSS package, release 12 (SPSS Inc., Chicago, IL, USA). Data are presented as mean value ± SD. Intergroup comparisons were performed using ANOVA. Pearson's correlation was used to evaluate univariate correlates of a given variable. Multivariable linear regression analyses were performed to examine the independent correlates between $DLCO_{sb}$ values and RV after adjusting for confounders such as age, LVEF and PASP. The null hypothesis was rejected at p≤0.05.

Table 2. Standard and advanced echocardiographic parameters of left ventricular systolic function.

Variable	IPF (n=33)	No-IPF (n=28)	p_a	Controls (n=30)	p_b	p_c
LV mass index (g/m²)	89.6±19.6	79.9±20.9	0.179	77.8±21.3	0.121	0.938
Relative wall thickness	0.38±0.05	0.38±0.06	0.996	0.36±0.06	0.605	0.568
LV EF (%)	61.1±4.9	63.5±4.9	0.230	62.5±4.9	0.624	0.786
LV GLS (%)	19.5±3.2	22.02±2.4	**0.003**	22.7±2.6	**<0.0001**	0.606
Transmitral E/Aratio	0.71±0.15	0.79±0.20	0.314	0.97±0.25	**<0.0001**	**<0.005**
E velocity DT (msec)	258.2±60.6	238.1±47.6	0.414	234.5±74.9	0.310	0.975
Septal e' velocity (cm/s)	6.0±2.0	7.0 ±2.0	0.241	9.0 ±3.0	**<0.0001**	**0.003**
Lateral e' velocity (cm/s)	8.0± 2.0	8.0 ±2.0	0.563	11.0 ±3.0	**<0.0001**	**<0.01**
E/e' ratio	10.2 ±4.4	8.7 ±1.9	0.146	7.5 ±2.0	**0.004**	0.336
LAVi (ml/m²)	25.5±7.6	23.8±5.5	0.608	25.7±6.4	0.985	0.539

p_a= IPF vs no-IPF, p_b = IPF vs controls, p_c = no-IPF vs controls

DT= Deceleration time, LAVi = Left atrial volume index, LV EF = Left ventricular ejection fraction, LV GLS = Left ventricular global longitudinal strain.
Other abbreviations as in Table 1

Table 3. Standard and advanced echo-Doppler parameters of right ventricular function.

Variable	IPF (n=33)	No-IPF (n=28)	p_a	Controls (n=30)	p_b	p_c
Standard Echo-Doppler						
RV basaltractdiameter (mm)	39.8±4.5	38.3±5.7	0.574	35.9±7.0	**0.028**	0.278
RV midtract diameter (mm)	32.6±5.9	30.7±5.9	0.387	29.3±4.6	**0.051**	0.579
RV longitudinaldiameter (mm)	64.2±7.7	61.4±7.6	0.391	61.5±8.7	0.409	0.998
TAPSE (mm)	20.9±2.9	22.4±3.4	0.165	23.4±3.2	**0.007**	0.453
Tricuspid E/A ratio	0.88±0.36	0.91±0.21	0.958	1.20±0.30	**<0.001**	**<0.002**
PASP (mmHg)	39.6±19.8	37.2±8.1	0.514	26.7±4.6	**0.002**	**0.047**
STE and 3D Echocardiography						
RV GLS (%)	20.0±2.6	22.1±2.8	**<0.05**	24.2±4.4	**<0.001**	**<0.05**
3D RV EDV (ml)	85.5±2.0	81.3±34.7	0.911	78.6±36.0	0.779	0.959
3D RV ESV (ml)	40.6±15.9	38.8± 16.6	0.928	33.3±18.3	0.320	0.495
3D SV (ml)	44.9 ± 18.5	42.6 ± 20.6	1.0	45.4 ± 19.0	1.0	1.0
3D RV EF (%)	50.5±9.9	50.9±7.6	0.987	59.1±6.9	**<0.002**	**<0.002**

p_a= IPF vs no-IPF,p_b= IPF vs controls, p_c= no-IPF vs controls.

RV= Right ventricular, TAPSE= Tricuspid annular plane systolic excursion, PASP = Pulmonary arterial systolic pressure, GLS= Global longitudinal strain,EDV=End-diastolic volume,EF= Ejection fractionESV=End- systolic volume.
Other abbreviations as in Table 1.

Results

Demographics, clinical features and main baseline heart and lung function parameters of the study population are summarized in **Table 1**. All ILD patients were free of cardiac symptoms/signs. Patients and healthy controls had similar age, while body mass index, heart rate and systolic BP were significantly higher in IPF patients than in controls. Lung function parameters did not differ between IPF and no-IPF patients.

LV standard echocardiographic and STE assessment are reported in **Table 2**. LV mass index, relative wall thickness and LA volume index were comparable between the three groups. Transmitral E/A ratio, septal and lateral e' velocity were significantly lower in IPF and no-IPF compared to controls. E/e' ratio was higher in the IPF group (p=0.004), but not in the no-IPF group, compared to controls. LV EF of both IPF and no-IPF did not differ significantly between and controls, whereas LV GLS was lower in IPF than in no-IPF (p= 0.003) and controls (p<0.0001).

The prevalence of PAH was 65% (n=21) in the IPF group and 75% (n=21) in the no IPF group but significative PAH (i.e., PASP> 50 mmHg) was observed only in 4 patients (12.5%) with IPF, and in 2 patients (7%) with no-IPF. RV standard and advanced STE and3D analysis is summarized in **Table 3**. Compared to healthy controls, IPF patients had larger RV transverse (p=0.028) and mid-cavity (p=0.051) diameters and lower TAPSE (p=0.007). Both IPF and no-IPF patients had lower tricuspid inflow E/A ratio (p<0.001 and p<0.002 respectively) and higher PASP (p<0.002 and 0.047 respectively) versus controls. Both IPF and no-IPF patients had also lower RV GLS in comparison with controls (p<0.001 and p<0.05 respectively) but RV GLS was also lower in IPF than in no-IPF (p<0.05). 3D-derived RV EF was lower in IPF and no-IPF compared to controls (both p<0.002) but did not differ significantly between the two ILDs groups (p=0.987). **Figure 1** depicts subgroup analysis showing the trend of RV GLS in IPF and no-IPF patients with and without PAH: notably, RV

GLS did not differ significantly between IPF with and without PAH and also between IPF without PAH and no-IPF with PAH.

<u>Univariate and multivariate associations</u>

In the pooled ILDS population $DLCO_{sb}$ was significantly related with RV GLS (r=0.55, p<0.0001) whereas the relation between LV GLS and $DLCO_{sb}$ was not significant (r=0.17, p=0.32) (**Figure 2**). RV GLS was not significantly related with pO_2 (r=0.03, p=0.83), pCO_2 (r=-0.26, p=0.08), FVC (r=0.04, p=0.79), and TLC (r=-0.01, p=0.96). Of note, RV GLS was also negatively related with PASP (r=-0.25, p=0.02). RV EF was not significantly related with any of the spirometric and pulmonary functional parameters.

By a multivariable regression performed In the pooled ILDs population, after adjusting for BMI, heart rate and PASP, $DLCO_{sb}$ was independently associated with RV GLS (standardized β coefficient = 0.583, p<0.0001). These results were substantially confirmed in IPF subgroup (β= 0.708, p<0.001) whilst no independent association between RV GLS and $DLCO_{sb}$ was found in the no-IPF population (**Table 4).**

Table 4. Independent determinants of RV GLS my multiple regression analyses.

a) In the overall ILDs population

Dependent variable	Covariate	B coefficient	p
RV GLS$_b$	BMI	-0.186	0.214
	HR	-0.027	0.851
	PASP	-0.053	0.712
	DLCO$_{sb}$	**0.583**	**<0.0001**

Cumulative R^2 = 0.575, SEE = 2.22%, p<0.007

b) In IPF subgroup

Dependent variable	Covariate	B coefficient	p
RV GLS	BMI	-0.267	0.139
	HR	-0.045	0.794
	PASP	-0.203	0.239
	DLCO$_{sb}$	**0.708**	**<0.001**

Cumulative R^2 = 0.729, SEE = 1.91 %, p=0.009

c) In no-IPF subgroup

Dependent variable	Covariate	B coefficient	p
RV GLS	BMI	-0.227	0.339
	HR	-0.190	0.536
	PASP	-0.304	0.277
	DLCO$_{sb}$	0.219	0.464

Cumulative R^2 = 0.603, SEE = 2.04 %, p=0.211

PF= Pulmonary fibrosis, IPF= idiopathic PF, DLCO $_{sb}$ = Single-breath lung diffusion capacity of carbon monoxide,PASP = Pulmonary arterial systolic pressure, RV=Right ventricular, GLS= Global Longitudinal Strain
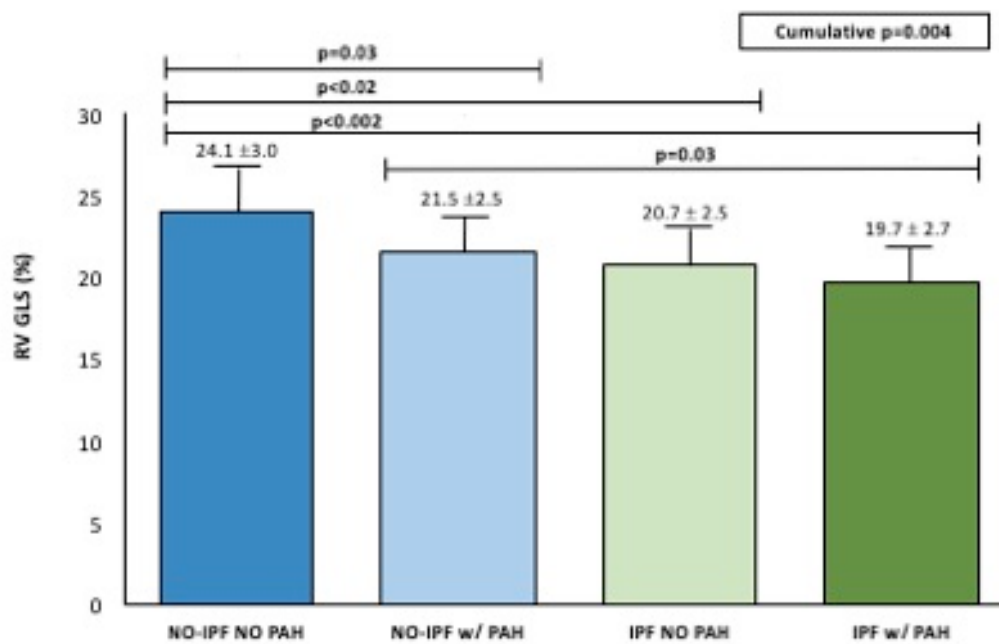
Figure 1. Behaviour of RV GLS (mean ± SD) in no-IPF and IPF without and with PAH.
RV GLS is significantly lower in IPF with or without PAH in comparison with both no-IPF groups.
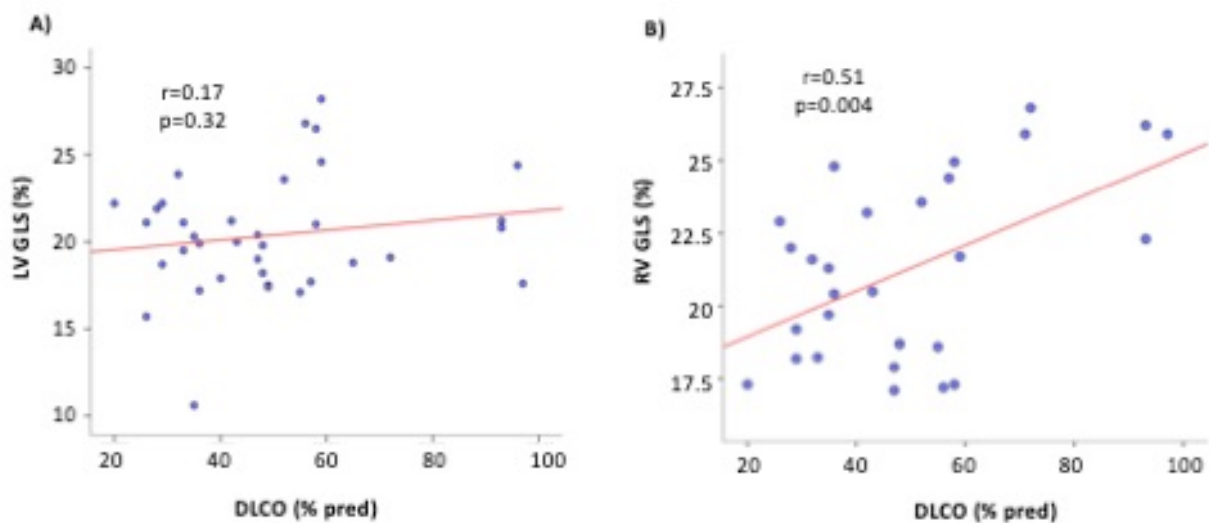
Figure 2. Scatterplot and regression line of the relation between DLCO and both LV GLS and RV GLS in the pooled ILDs population.
The relation of RV GLS - but not of LV GLS - is significant

Discussion

To the best of our knowledge, the present study is the first to compare LV and RV echocardiographic features of IPF and no-IPF ILDs patients without evidence of any other heart disease, in relation with a healthy control group. Our findings demonstrate that IPF present

(I) LV diastolic dysfunction – which is detectable even in no-IPF patients – and a subclinical LV systolic dysfunction, testified by the reduction of LV GLS but not of LV EF, which cannot be observed in no-IPF patients,

(II) a clear alteration of RV geometry and both systolic (RV EF and GLS) and diastolic function, and a substantial PASP increase in comparison with controls whereas no-IPF patients present only an alteration of RV diastolic dysfunction and a lower degree of PASP increase.

Moreover, (III) an independent association between $DLCO_{sb}$ and RV longitudinal dysfunction is found in the pooled ILDs population, it being evident in IPF but not in no-IPF group.

LV diastolic and systolic function

LV diastolic dysfunction, characterized by a reduction of transmitral E/A ratio and e' mitral annular velocity and increase of E/e' ratio, was already observed in IPF patients [8]. Our data confirm this impairment of LV filling (lower E/A ratio) and of myocardial relaxation (lower Tissue Doppler septal and lateral e' velocity) and the higher E/e' ratio in IPF than in the healthy controls. According to the ASE/EACVI recommendations [21], these findings provide evidence of a variable degree of LV diastolic dysfunction and a trend to LV filling pressures increase in IPF patients. Despite with a lower extent, the same diastolic abnormalities were observed also in non-IPF patients, highlighting a likely process of ventricular diastolic interdependence in all ILDs population. Ventricular interdependence corresponds to the forces transmitted from the left ventricle to the other and viceversa through the myocardium and pericardium and occurs because

the two ventricles have common myocardial fibers, share the interventricular septum and are wrapped within the pericardium [29]. Accordingly, diastolic function of right ventricle can influence that of the left ventricle by several mechanisms including RV pressure overload [30,31]. However, in the present study LV diastolic alterations of both IPF and no IPF were evident in presence as in absence of PAH and cannot be therefore ascribed to an impairment of LV myocardial relaxation occurring as the consequence of septal wall distorsion towards the left ventricle due to RV pressure overload [30,32,33]. It is also worthy of note that only in IPF patients LV GLS, but not LV EF, was significantly lower in comparison with both healthy controls and no-IPF. This finding is confirmatory of a previous report of D'Andrea et al in IPF [10] and extends the interdependence phenomenon of IPF to LV longitudinal systolic function. It is conceivable that in this clinical setting LV systolic involvement could be functional rather than related to structural LV changes as LV mass and relative wall thickness did not differ significantly from controls and no-IPF. This concept is indirectly testified by the reversibility on relief of the RV pressure overload occurring in ILDs patients after lung transplantation [34].

RV size and function

RV abnormalities of RV have been demonstrated to be evident and predict prognosis in IPF. In a retrospective study on 135 IPF patients referred for lung transplantation, increased RV/LV ratio, right atrial and RV dilation, and moderate to severe RV dysfunction (TAPSE <1.6 cm) were all associated with an increased risk of death, independently of lung function parameters [7]. RV abnormalities appear to be mainly due to PAH, which has a high prevalence (till 85%) in the advanced disease stages [35]. In IPF patients of less advanced stages (with normal TAPSE and LV EF), D'Andrea et al. showed a significant reduction of RV strain, as an index of early impairment of RV systolic function [9]. RV GLS was also a powerful independent determinant of functional capacity during 6-minute walking test and a cut-off value of RV GLS ≤12% emerged as an

independent predictor of cardiac outcome at 19 months follow-up, even in absence of PAH [10]. In the present study, both IPF and no-IPF patients had lower tricuspid inflow E/A ratio, higher PASP and lower RV GLS compared to controls. However, a significant difference in RV size (increased RV transverse basal and mid-cavity diameters) and function (reduced TAPSE) was found only in the IPF when compared to controls. Among the different echocardiographic parameters investigated, only RV GLS differentiated the two ILDs subgroups, it being significantly lower in IPF than in no-IPF. Of note, this diagnostic ability was own of RV GLS but not of 3D-derived RV EF which was significantly reduced in both IPF and no-IPF in comparison with healthy controls. This finding is completely new and provides evidence of the additional diagnostic capabilities of RV strain imaging in ILDs. It is conceivable that microvascular injury, largely demonstrated as an early stages of IPF lungs [36], could be extended also to RV subendocardial layer, of which GLS is a reliable marker [37].

Univariate and multivariate associations provided additional insights. The association between DLCOsb reduction and RV GLS impairment, found in the pooled ILDs and in IPF but not in no-IPF, was independent on confounders such as body mass index, heart rate and PASP. DLCOsb is an index of the IPF disease status [38], represents an independent predictor of mortality in patients with ILD and can be used therefore for risk stratification in this clinical setting [38-40]. It is conceivable therefore that the impairment of RV longitudinal function in IPF patients could be essentially due to a reduced gas exchange between alveoli and capillary blood stream.

Study Limitations

First of all, despite realized in a highly specialized reference setting, the present study is representative of the effort of a single center with a small sample size of ILDs. As we mainly focused on IPF and smoke-related no-IPF pneumonias, our results certainly do not allow to drive definite considerations in other forms of no-IPF including those related to connective tissue

diseases. Indeed, patients with connective tissue diseases derived fibrotic ILDs likely merits separate analysis because of their high frequency of concomitant pulmonary vascular involvement [41,42]. In addition, our findings cannot be extrapolated to patients with the most advanced lung fibrosis, as most of our IPF patients were affected by mild to moderate disease. Further efforts in larger populations with more advanced IPF stages should therefore be encouraged in a multi-center setting.

Another limitation could correspond to the use of DLCO. Unlike FVC, DLCO changes are not specific as they depend on both ventilation and perfusion and are expression of the integrity of the alveolar-capillary membrane. In addition, DLCO has a marked within-session and inter-session variability [Ref]. Nevertheless, DLCO is widely recognized as a surrogate measure of pulmonary fibrosis extent and its changes have been demonstrated to be predictive of IPF disease progression over a 12-month periods [3].

Conclusions

The findings of the present study point out the diagnostic capabilities of strain imaging in distinguishing early cardiac damage of IPF from and no-IPF patients, a task which cannot be attributed to both standard and 3D echo. RV GLS is a novel key parameter for detecting early cardiac damage in ILDs, with likely prognostic power, in this clinical scenario. Future studies could be addressed to investigate if RV GLS alterations are also associated with fibrotic heart rearrangement [43].

Table 1. Clinical features and baseline heart and lung function parameters of the study population.

Variable	IPF (n=33)	No- IPF (n=28)	p_a	Controls (n=30)	p_b	p_c
Gender (F/M)	6/27	10/18	-	11/19	-	-
Age (years)	70.1 ± 7.6	65.2 ± 8.1	0.067	66.9 ± 8.7	0.375	1.0
BMI (kg/m^2)	27.8 ± 3.8	30.1 ± 4.0	0.068	25.2 ± 3.2	**0.015**	**<0.0001**
Systolic BP (mmHg)	138.8 ± 18.6	133.7 ± 15.2	0.642	128.4 ± 12.5	**0.033**	0.618
Diastolic BP (mmHg)	78.9 ± 12.2	77.5 ± 9.8	1.0	78.7 ± 9.3	1.0	1.0
Heart rate (bpm)	76.8 ± 11.5	75.7 ± 10.9	1.0	68.2 ± 11.1	**0.009**	**0.039**
PaO_2(mm Hg) in ambient air	71.6 ± 10.1	73.1 ±8.7	0.548	-	-	-
$PaCO_2$(mm Hg) in ambient air	39.7 ± 3.7	38.1±3.0	0.327	-	-	-
FVC (%pred)	71.1 ± 20.9	70.6±19.4	0.227	-	-	-
TLC (%pred)	70.9 ± 47.8	70.1±25.9	0.368	-	-	-
DLCO$_{sb}$(%pred)	44.3 ± 17.6	54.7 ±22.3	0.242	-	-	-

p_a= IPF vs non-IPF, p_b= IPF vs controls, $p_{c:}$= non- IPF vs controls.

IPF = Idiopathic pulmonary fibrosis, BMI = body mass index, BP = Blood pressure, PaO_2 = Arterial oxygen partial pressure, $PaCO_2$ = Arterial carbon dioxide partial pressure, FVC % = Forced vital capacity, FEV1% = Forced expiratory volume in 1 s, TLC = Total lung capacity; DlCO $_{sb}$ = Single-breath lung diffusion capacity of carbon monoxide.

References

1. Mikolasch, T.A.; Garthwaite, H.S.; Porter, J.C. Update in diagnosis and management of interstitial lung disease. *Clin Med* **2016**,*16*,71-78.
2. Raghu, G.; Weycker, D.; Edelsberg, J.; Bradford, W.Z.; Oster, G. Incidence and prevalence of idiopathic pulmonary fibrosis. *Am J Respir Crit Care* **2006**,*174*, 810-816.
3. Raghu, G.; Collard, H.R.; Egan, J.J.; Martinez, F.J.; Behr, J.; Brown, K.K.; Colby, T.V.; Cordier, J.F.; Flaherty, K.R.; Lasky, J.A.; et al. ATS/ERS/JRS/ALAT Committee on Idiopathic Pulmonary Fibrosis. An official ATS/ERS/JRS/ALAT statement: idiopathic pulmonary fibrosis: evidence-based guidelines for diagnosis and management. *Am J Respir Crit Care Med* **2011**,*183*,788-824.
4. Raghu, G.; Amatto, V.C.; Behr, J.; Stowasser, S. Comorbidities in idiopathic pulmonary fibrosis patients: a systematic literature review. *Eur Respir J* **2015**,*46*,1113-1130.
5. Kreuter, M.; Ehlers-Tenenbaum, S.; Palmowski, K.; Bruhwyler, J.; Oltmanns, U.; Muley, T.; Heussel, C.P.; Warth, A.; Kolb, M.; Herth, F.J. Impact of comorbidities on mortality in patients with idiopathic pulmonary fibrosis. *PLoS ONE* **2016**,*11*, e0151425.
6. Kimura, M.; Taniguchi, H.; Kondoh, Y.; Kimura, T.; Kataoka, K.; Nishiyama, O.; Aso, H.; Sakamoto, K.; Hasegawa, Y. Pulmonary hypertension as a prognostic indicator at the initial evaluation in idiopathic pulmonary fibrosis. *Respiration* **2013**,*85*,456-463.
7. Rivera-Lebron, B.N.; Forfia, P.R.; Kreider, M.; Lee, J.C.; Holmes, J.H.; Kawut, S.M. Echocardiographic and hemodynamic predictors of mortality in idiopathic pulmonary fibrosis. *Chest* **2013**,*144*,564-570.
8. Papadopoulos, C.E.; Pitsiou, G.; Karamitsos, T.D.; Karvounis, H.I.; Kontakiotis, T.; Giannakoulas, G.; Efthimiadis, G.K.; Argyropoulou, P.; Parharidis, G.E.; Bouros, D. Left ventricular diastolic dysfunction in idiopathic pulmonary fibrosis: a tissue Doppler echocardiographic study. *Eur Respir J **2008**, 31*,701-706.
9. D'Andrea, A.; Stanziola, A.; D'Alto, M.; Di Palma, E.; Martino, M.; Scarafile, R.; Molino, A.; Rea, G.; Maglione, M.; Calabrò, R.; et al. Right ventricular strain: an independent predictor of survival in idiopathic pulmonary fibrosis. *Int J Cardiol* **2016**,*222*,908-910.
10. D'Andrea, A.; Stanziola, A.; Di Palma, E.; Martino, M.; D'Alto, M.;Dellegrottaglie, S.; Cocchia, R.;Riegler, L.; Betancourt Cordido, M.V.; Lanza, M.;et al. Right ventricular structure and function in idiopathic pulmonary fibrosis with or without pulmonary hypertension. *Echocardiography* **2016**,*33*,57-65.
11. Miller, M.R.; Hankinson, J.; Brusasco, V.; Burgos, F.; Casaburi, R.; Coates, A.; Crapo, R.; Enright, P.; Van der Grinten, C.P.; Gustafsson, P.; et al. ATS/ERS Task Force. Standardisation of spirometry. *Eur Respir J.***2005**,*26*,319-38.
12. Wanger, J.; Clausen, J.L.; Coates, A.; Pedersen, O.F.; Brusasco, V.; Burgos, F.; Casaburi, R.; Crapo, R.; Enright, P.; Van der Grinten, C.P.; et al. Standardisation of the measurement of lung volumes. *Eur Respir J*. **2005**,*26*,511-22.
13. Macintyre, N.; Crapo, R.O.; Viegi, G.; Johnson, D.C.; van der Grinten, C.P.; Brusasco, V.; Burgos, F.; Casaburi, R.; Coates, A.; Enright, P.; et al. Standardisation of the single-breath determination of carbon monoxide uptake in the lung. *Eur Respir J*. **2005**,*26*,720-35.
14. ATS Committee on Proficiency Standards for Clinical Pulmonary Function Laboratories.ATS statement: guidelines for the six-minute walk test. *Am J Respir Crit Care Med* **2002**,*166*,111-117.
15. Esposito, R.;Galderisi, M.;Schiano-Lomoriello, V.; Santoro, A.; De Palma, D.; Ippolito, R.; Muscariello, R.; Santoro, C.; Guerra, G.;Cameli, M.;et al. Non symmetric myocardial

contribution to supranormal right ventricular function in the athlete's heart: combined assessment by speckle tracking and real time three-dimensional echocardiography. *Echocardiography* **2014**,*31*, 996-1004.

16.   Horton, K.D.; Meece, R.W.; Hill, J.C. Assessment of the right ventricle by echocardiography: a primer for cardiac sonographers. *J Am Soc Echocardiogr* **2009**;*22*,776-792.

17.   Niemann, P.S.; Pinho, L.; Balbach, T.; Galuschky, C.; Blankenhagen, M.; Silberbach, M.; Broberg, C.; Jerosch-Herold, M.; Sahn, D.J. Anatomically oriented right ventricular volume measurements with dynamic three-dimensional echocardiography validated by 3-Tesla magnetic resonance imaging. *J Am Coll Cardiol* **2007**,*50*,1668-1776.

18.   Galderisi, M.; Cosyns, B.; Edvardsen, T.; Cardim, N.; Delgado, V.; Di Salvo, G.; Donal, E.; Sade, L.E.; Ernande, L.; Garbi, M.; et al. 2016–2018 EACVI Scientific Documents Committee; 2016–2018 EACVI Scientific Documents Committee. Standardization of adult transthoracic echocardiography reporting in agreement with recent chamber quantification, diastolic function, and heart valve disease recommendations: an expert consensus document of the European Association of Cardiovascular Imaging. *Eur Heart J Cardiovasc Imaging* **2017**,*18*,1301-1310.

19.   Lang, R.M.; Badano, L.P.; Mor-Avi, V.; Afilalo, J.; Armstrong, A.; Ernande, L.; Flachskampf, F.A.; Foster, E.; Goldstein, S.A.; Kuznetsova, T.; et al. Recommendations for cardiac chamber quantification by echocardiography in adults: an update from the American Society of Echocardiography and the European Association of Cardiovascular Imaging. *Eur Heart J Cardiovasc Imaging* **2015**,*16*,233–270.

20.   Rudski, L.G.; Lai, W.W.; Afilalo, J.; Hua, L.; Handschumacher, M.D.; Chandrasekaran, K.; Solomon, S.D.; Louie, E.K.; Schiller, N.B. Guidelines for the echocardiographic assessment of the right heart in adults: a report from the American Society of Echocardiography endorsed by the European Association of Echocardiography, a registered branch of the European Society of Cardiology, and the Canadian Society of Echocardiography. *J Am Soc Echocardiogr* **2010**, *23*,685-713.

21.   Nagueh, S.F.; Smiseth, O.A.; Appleton, C.P.; Byrd, B.F. 3rd; Dokainish, H.; Edvardsen, T.; Flachskampf, F.A.; Gillebert, T.C.; Klein, A.L.; Lancellotti, P.; et al. Recommendations for the evaluation of left ventricular diastolic function by echocardiography: an update from the American Society of Echocardiography and the European Association of Cardiovascular Imaging. *Eur Heart J Cardiovasc Imaging* **2016**,*17*,1321-1360.

22.   Lembo, M.; Esposito, R.; Lo Iudice, F.; Santoro, C.; Izzo, R.; De Luca, N.; Trimarco, B.; De Simone, G.; Galderisi, M. Impact of pulse pressure on left ventricular global longitudinal strain in normotensive and newly diagnosed, untreated hypertensive patients. *J Hypertens* **2016**, *34*,1201-1207.

23.   Santoro, C.; Esposito, R.; Lembo, M.; Sorrentino, R.; De Santo, I.; Luciano, F.; Casciano, O.; Giuliano, M.; De Placido, S.;Trimarco, B.;et al. Strain-oriented strategy for guiding cardioprotection initiation of breast cancer patients experiencing cardiac dysfunction. *Eur Heart J Cardiovasc Imaging* **2019**,*20*,1345-1352.

24.   Alcidi, G.M.; Esposito, R.; Evola, V.; Santoro, C.; Lembo, M.; Sorrentino, R.; Lo Iudice, F.; Borgia, F.; Novo, G.;Trimarco, B.;et al. Normal reference values of multilayer longitudinal strain according to age decades in a healthy population: a single-centre experience. *Eur Heart J Cardiovasc Imaging* **2017**,*19*,390–1396.

25.   Cameli, M.; Lisi, M.; Righini, F.M.; Tsioulpas, C.; Bernazzali, S.; Maccherini, M.; Sani, G.; Ballo, P.; Galderisi, M.; Mondillo, S. Right ventricular longitudinal strain correlates well with

right ventricular stroke work index in patients with advanced heart failure referred for heart transplantation. *J Card Fail* **2012**,*18*,208-15.

26.   Maffessanti, F.; Muraru, D.; Esposito, R.; Gripari, P.; Ermacora, D.; Santoro, C.; Tamborini, G.; Galderisi, M.; Pepi, M.; Badano, L.P. Age-, body size-, and sex-specific reference values for right ventricular volumes and ejection fraction by three-dimensional echocardiography: a multicenter echocardiographic study in 507 healthy volunteers. *Circ Cardiovasc Imaging* **2013**,*6*,700-10.

27.   Buonauro, A.;Galderisi, M.; Santoro, C.; Canora, A.; Bocchino, M.L.; Lo Iudice, F.; Lembo, M.; Esposito, R.; Castaldo, S.;Trimarco, B.; et al. Obstructive sleep apnoea and right ventricular function: A combined assessment by speckle tracking and three-dimensional echocardiography. *Int J Cardiol* **2017,**243,544-549.

28.   Leibundgut, G.; Rohner, A.; Grize, L.; Bernheim, A.; Kessel-Schaefer, A.; Bremerich, J.; Zellweger, M.; Buser, P.; Handke, M. Dynamic assessment of right ventricular volumes and function by real-time three-dimensional echocardiography: a comparison study with magnetic resonance imaging in 100 adult patients. *J Am Soc Echocardiogr* **2010,**23,116-126.

29.   Santamore, W.P., Dell'Italia, L.J. Ventricular interdependence: significant left ventricular contributions to right ventricular systolic function. *Progr Cardiovasc Dis* **1998**; 40, 289–308.

30.   Morris-Thurgood, J.; Frenneaux, M. Diastolic ventricular interaction and ventricular diastolic filling. *Heart Fail Rev* **2000**,*5*,307–323.

31.   Lazar, J.M.; Flores, A.R.; Grandis, D.J.; Orie, J.E.; Schulman, D.S. Effects of chronic right ventricular pressure overload on left ventricular diastolic function. *Am J Cardiol* **1993,** *72*, 1179–1182.

32.   Lavine, S.J.; Tami, L.; Jawad, I. Pattern of left ventricular diastolic filling associated with right ventricular enlargement. *Am J Cardiol* **1988**, *62*,444–448.

33.   Louie, E.K.; Rich, S.; Levitsky, S.; Brundage, B.H. Doppler echocardiographic demonstration of the differential effects of right ventricular pressure and volume overload on left ventricular geometry and filling. *J Am CollCardiol***1992,**19,84–90.

34.   Jastrzebski, D.; Nowak, J.; Ziora, D.; Wojarski, J.; Czyzewski, D.; Kozielski, J.; Polonski, L.; Zembala, M. Left ventricular dysfunction in patients with interstitial lung diseases referred for lung transplantation. *J Physiol Pharmacol* **2007**,*58*,299–305.

35.   Patel, N.M.; Lederer, D.J.; Borczuk, A.C.; Kawut, S.M. Pulmonary hypertension in idiopathic pulmonary fibrosis. *Chest* **2007**,*132*,998-1006.

36.   Calabrese, F.; Giacometti, C.; Rea, F.; Loy, M.; Valente, M. Idiopathic interstitial pneumonias: Primum movens: epithelial, endothelial or whatever. *Sarcoidosis Vasc Diffuse Lung Dis* **2005**, *22*,S15-s23.

37.   Mor-Avi, V.; Lang, R.M.; Badano, L.P.; Belohlavek, M.; Cardim, N.M.; Derumeaux, G.; Galderisi, M.; Marwick, T.; Nagueh, S.F.; Sengupta, P.P.; et al. Current and evolving echocardiographic techniques for the quantitative evaluation of cardiac mechanics: ASE/EAE consensus statement on methodology and indications endorsed by the Japanese Society of Echocardiography. *Eur J Echocardiogr* **2011**,*12*,167-205.

38.   Hamada, K.; Nagai, S.; Tanaka, S.; Handa, T.; Shigematsu, M.; Nagao, T.; Mishima, M.; Kitaichi, M.; Izumi, T. Significance of pulmonary arterial pressure and diffusion capacity of the lung as prognosticator in patients with idiopathic pulmonary fibrosis. *Chest* **2007,**131,650-656.

39.   Yasui, K.; Yuda, S.; Abe, K.; Muranaka, A.; Otsuka, M.; Ohnishi, H.; Hashimoto, A.; Takahashi, H.; Tsuchihashi, K.; Takahashi, H.; et al. Pulmonary vascular resistance estimated by Doppler echocardiography predicts mortality in patients with interstitial lung disease. *J Cardiol* **2016**,*68*,300-307.

40.	Kimura, M.; Taniguchi, H.; Kondoh, Y.; Kimura, T.; Kataoka, K.; Nishiyama, O.; Aso, H.; Sakamoto, K.; Hasegawa, Y. Pulmonary hypertension as a prognostic indicator at the initial evaluation in idiopathic pulmonary fibrosis. *Respiration* **2013**, *85,*456-463.

41.	Lindqvist, P.; Caidahl, K.; Neuman-Andersen, G.; Ozolins, C.; Rantapää-Dahlqvist, S.; Waldenström, A.; Kazzam, E. Disturbed right ventricular diastolic function in patients with systemic sclerosis: a Doppler tissue imaging study. *Chest* **2005,** *128,*755–763.

42.	Gin, P.L.; Wang, W.C.; Yang, S.H.; Hsiao, S.H.; Tseng, J.C. Right heart function in systemic lupus erythematosus: insights from myocardial Doppler tissue imaging. *J Am Soc Echocardiogr* **2006,***19,*441–449.

43.	Kisseleva, T.; Brenner, D.A. Fibrogenesis of parenchymal organs. *Proc Am Thorac Soc* **2008**,*5,*338-342.